The Properties and Morphologies of Composites Based on Sulfated EPDM Ionomer Toughed Polypropylene Highly Filled with Mg(OH)$_2$

Zhanipai Su, Pingkai Jiang, Qiang Li, Ping Wei

School of Chemistry and Chemical Engineering, Shanghai Jiao Tong University, Shanghai 200240, China

ABSTRACT: PP was endowed with excellent flame retardant properties by great mount of Mg(OH)$_2$ particulates. It was found that the mechanical properties of PP was severely deteriorated, caused by the bad compatibility between filler and matrix, as well as the agglomerate of Mg(OH)$_2$ particles in PP matrix. The addition of rubbery phase as the third component could remarkably improve the Izod impact strength of PP highly filled inorganic flame retardant agent. In this article, EPDM and sulfated EPDM ionomer were adopted as the third component to improve the mechanical properties of PP/Mg(OH)$_2$ composites. The composites have better mechanical properties using sulfated EPDM ionomer as the third component than that of neat EPDM. The theoretical analysis and SEM photographs showed that even dispersion of particulates and the less domain size of rubbery phases as well as the better adhesion between rubbery phase and PP matrix were the main reasons for the improvement of the mechanical properties. © 2006 Wiley Periodicals, Inc. J Appl Polym Sci 102: 295–302, 2006

Key words: ionomer; polypropylene; flame retardance; morphology

INTRODUCTION

Composites represent an important class of engineering materials. The incorporation of mineral fillers into thermoplastics has been widely practiced in industry to extend them and to enhance certain properties.[1–3] Polypropylene has been widely used in electrical products, mechanical equipment, and other fields. Adopting flame retardant system could extend its application in many fields. As a rule, intumescent flame retardant (IFR) systems are generally used in polypropylenes because of their high efficiency and low dose levels, as polypropylene has bad compatibility with inorganic fillers, but IFRs have the drawbacks of low decomposition temperatures and easy absorption of water. The processing temperature of polypropylene is often over 200°C, so using Mg(OH)$_2$ or one of the grades of Al(OH)$_3$ with a high decomposition temperature as the flame retardant system in polypropylene to replace IFRs is a popular trend.[4–6]

Unfortunately, the high loading of Mg(OH)$_2$ required in PP leads to a reduction in impact strength and elongation at break, due primarily to the poor interfacial adhesion between the two components.[7–9] PP is a typical pseudoductile polymer. It possesses a much higher crack initiation resistance than crack propagation resistance, which leads to a high unnotched but a low notched impact strength. Rubber is often used as the third component to improve the mechanical properties of the composites, according to cavitation/debonding and shear-yielding mechanisms.[10–14]

The incorporation of ionic groups into organic polymers yields ionomers. The presence of small amount of ionic groups exerts profound effect on the physical properties of the polymer. The special structure of ionomer with polar groups attaching on nonpolar main chain makes it have favorable adhesion both PP matrix and Mg(OH)$_2$ particulate.[15–19] It is not difficult to predict that, using the ionomer elastomer as the third component, the composites will possess excellent tensile properties beside the good notched impact strength.

In the present study, the ionomer elastomer of zinc neutralized sulfated EPDM (Zn-SEPDM) was synthesized. The mechanical and retardant properties of the flame retardant thermoplastic based on Polypropylene filled with Mg(OH)$_2$ were studied. EPDM and Zn-SEPDM were used as the third component to modify the impact toughness and tensile properties of PP filled with Mg(OH)$_2$; The limiting oxygen index (LOI) was used to analyze the flame retardant properties; Fourier transform infrared spectroscopy (FTIR) was used to characterize the Zn-SEPDM, and SEM was used to analyze the mechanism of toughening.
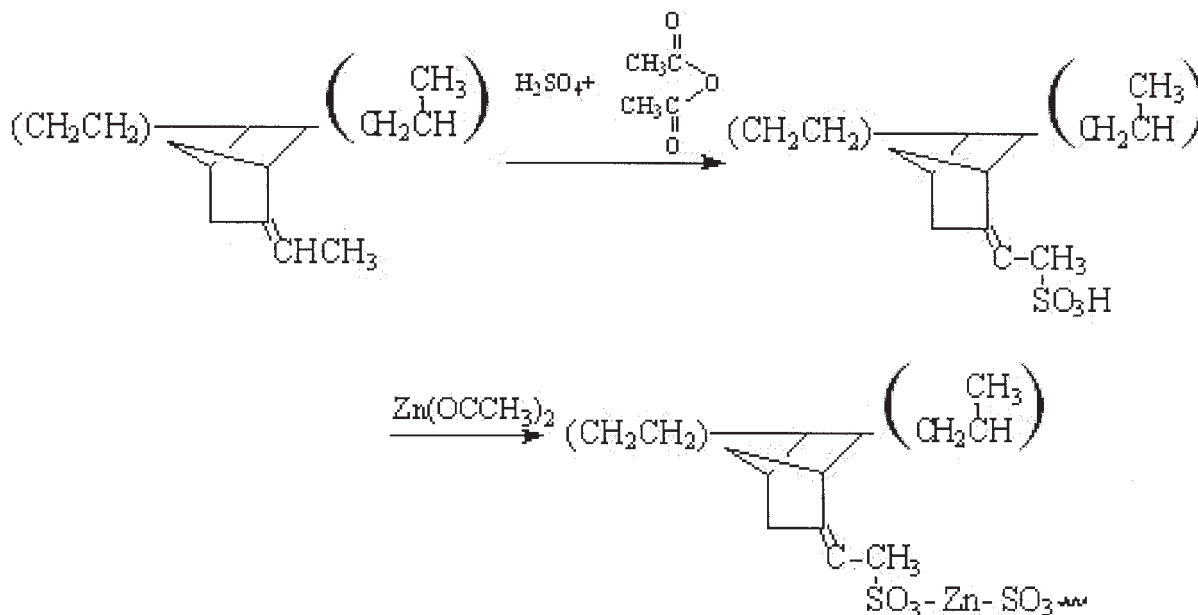
Correspondence to: P. Jiang (pkjiang@sjtu.edu.cn).

Figure 1 Reaction equation of zinc neutralized sulfated EPDM.

EXPERIMENTAL

Materials

The polypropylene was isotactic (iPP) Novatel H57541 (M_w = 300,000 by gel permeation chromatography, GPC) supplied by the Japan Polychem Corp. with a density of 0.90 g/cm^3 and a melt flow index of 3.7 g/10 min (GB 3682–83). The EPDM was Novadel IP 4770R supplied by the DuPont Dow Corp. (Mooney Viscosity, ASTM D 1646, ML 1 + 4 at 125°C: 70; Typical Molecular Weight, M_w = 200,000, by GPC; The mass ratio of Ethylene = 70% by ASTM D 3900; The mass ratio of Ethylidene Norbornene (ENB) = 4.9 by ASTM D 6047; MWD Characteristics is Medium according to DuPont Dow Method: EPRG-2). Zinc acetate (AR), sulfuric acid (AR), and acetic anhydride were supplied by the Shanghai Chemical Reagent Co. (China). Mg(OH)$_2$ powder of mean particle size of 0.4 mm and nitrogen surface area of 15 m^2/g (BET method) and the compact density is 2.2 g/cm^3 was provided by Sou Le Enterprise Co., Ltd., Hong Kong.

Preparation of zinc neutralized sulfated EPDM

Acetyl sulfate preparation: First, 50 mL acetic anhydride was cooled below –10°C, and 50 mL of 96% sulfuric acid was added. The solution was stirred, and 1,2-dichloroethane (DCE) was added. The product obtained was maintained at 0°C in an ice bath, until its addition to the reaction medium.

Sulfonation reaction: Sulfonation was carried out according to the procedure described by Makowski et al.[19–21] In an agitated reactor, the polymer was dissolved in cyclohexane at 60–70°C and purged with

nitrogen. Then acetyl sulfate, prepared as described earlier, was added. The solution was stirred and purged with nitrogen during the experiment. The reaction was terminated by precipitating in methanol or water after the desired reaction time.

Neutralization reaction: Neutralization was carried out after the earlier mentioned sulfonation reaction was terminated. Then the solution was stirred and precipitated in the extra zinc sulfate solution of ethanol and water, and purged with nitrogen during the experiment. After the desired reaction time, the product was obtained.

The equation for the reactions is shown in Figure 1.

The complete removal of residual acid and salt after neutralization is important because it can interfere with the properties of the final product. The dried polymer was cut into small pieces, washed once with boiling deionized water, and then again many times with cold water until a neutral pH of sewage was obtained. It was finally vacuum-dried at 70°C for 3 days.

Sample preparation

A certain amount of PP, EPDM, or Zn-SEPDMS-EPDM were mixed in a HAAKE Rheocord 90 internal mixer at 170°C and 80 rpm, after which Mg(OH)$_2$ was added after 5 min and the total volume were kept as 60–70 cm^3. The samples were obtained when the torque reached a constant value. After mixing, the composites were compression molded into plaques 1 mm and 3 mm thick, at a temperature of 170°C and 10 MPa for 5 min.
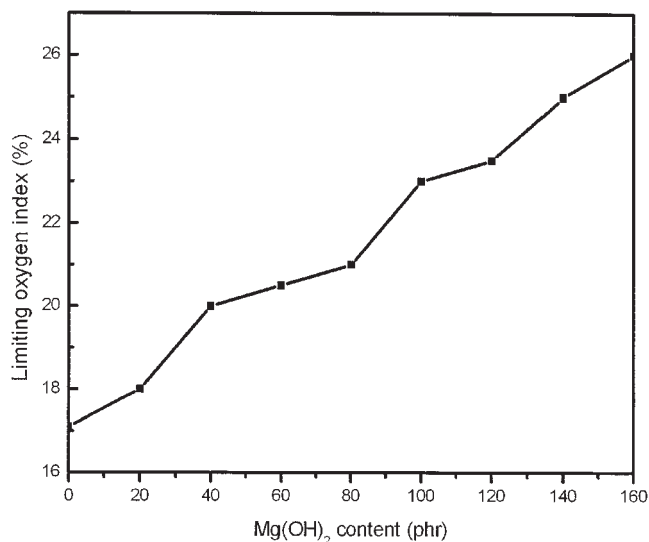
Figure 2 Limiting oxygen index of composites of polypropylene filled with various amount of $Mg(OH)_2$ samples.

Characterization

Flammability

Specimens used for the test ($100 \times 6.5 \times 3$ mm^3) (were cut from 3-mm thick compression-molded sheets. Flammability behavior was characterized by measuring the limiting oxygen index (LOI) using a Stanton-Redcroft LOI FTA type instrument (Rheometric Scientific Ltd., UK), according to ASTM D 2863.

Mechanical properties

Tensile dumbbell specimens were cut from the 1 mm thick sheets and tested using an Instron 4465 tensile tester, according to ISO 527 at a crosshead speed of 50 mm/min. Specimens ($63.5 \times 12.7 \times 3$ mm^3) were cut from the compression-molded sheets. A 0.25 mm notch was machined in all specimens, which were then checked for notch defects. Notched specimens were tested in a Ray–Ran impact tester, according to ISO 8256 at a hammer speed of 3.5 m/s and a pendulum weight of 0.818 Kg.

Fourier transform infrared spectroscopy

First, the samples obtained were pressed into films 100 mm thick. Infrared transmission spectra were obtained using an FTIR spectrometer, Model Paragon 1000 from Perkin–Elmer Corp. (USA) with a resolution of 4 cm^{-1}.

Morphology observation

The phase morphology of the composites was examined by scanning electron microscopy of fracture sur-

faces (Hitachi S520 SEM). Specimens were prepared by immersing test pieces in liquid nitrogen before breaking. For morphological analysis, cryogenically fractured specimens etched by the mixed solution of sulfated acid, phosphate acid, and dichromic acid at 70°C for 5 min to remove the EPDM or Zn-SEPDM phase. The fractured surfaces were coated with gold before examination.

RESULTS AND DISCUSSION

Effect of $Mg(OH)_2$ content on the flammability of the $PP/Mg(OH)_2$ composites

The dependence of the LOI of $PP/Mg(OH)_2$ samples on $Mg(OH)_2$ content was shown in Figure 2. As the results reported previously,[4–6] the LOI of the samples improved with increasing filler content, and the LOI of the neat PP and the PP filled with 150 phr $Mg(OH)_2$ were 17 and 25.5, respectively. This demonstrates that $Mg(OH)_2$ is a kind of flame retardant agent with relatively low efficiency. A great amount of $Mg(OH)_2$ is needed to obtain the flame retardant material.

Effect of $Mg(OH)_2$ content on the mechanical properties of $PP/Mg (OH)_2$ composites

The effect of $Mg(OH)_2$ content on the mechanical properties of the $PP/Mg(OH)_2$ composites illustrated in Figures 3 and 4. The mechanical properties will decrease with increasing levels of $Mg(OH)_2$ for PP and $Mg(OH)_2$ are not compatible. When the filler loading reached 150 phr, the elongation at break, stress at break and Izod impact strength reduced to the unacceptably low levels of 2%, 10 MPa and 1 kJ/m^2, respectively.

Impact strength is often used as the measure of toughness because it is relatively simple to perform. As semicrystalline engineering thermoplastics, PP
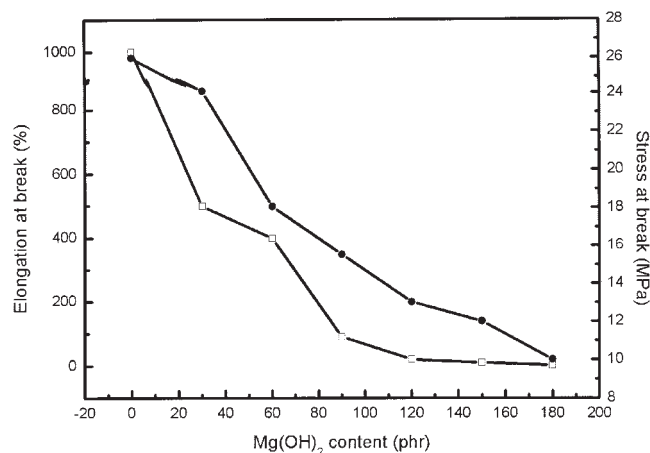

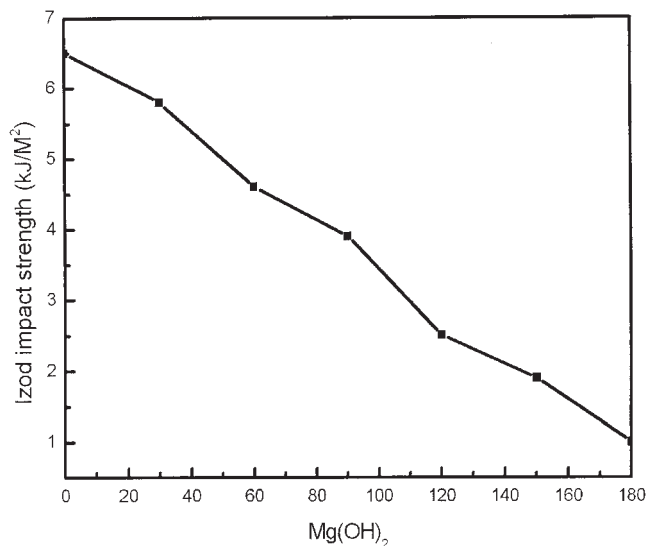**Figure 3** The tensile properties of the PP filled with various amount of $Mg(OH)_2$.

Figure 4 The notched Izod impact strength of the PP filled with various content $Mg(OH)_2$.

possesses a much higher crack initiation resistance than crack propagation resistance, leading to high unnotched but low notched impact strength. Because of weak interface adhesion between the filler and the PP matrix, there is no load transfer and the total load is carried by the divided PP matrix. The notched Izod impact strength of the $PP/Mg(OH)_2$ composites will decrease with increasing the concentration of $Mg(OH)_2$ particles.

The tensile properties of composites and blends are depended on the interfacial adhesion to a great extent. Neilsen's simple model for perfect adhesion is often used to evaluate the adhesion of particle filled polymer composites[22,23]:

$$\frac{\varepsilon}{\varepsilon_0} = 1 - \phi^{1/3} \tag{1}$$

where ε and ε_0 represent the elongation at break of the composite and of the neat PP, respectively, and ϕ is the volume fraction of $Mg(OH)_2$ in the composites.

Figure 4 compared the theoretical values by Neilsen's model with the experimental values of the elongation at break. It can be seen that the experimental values were lower than predicted values. It indicated the bad adhesion between the $Mg(OH)_2$ particles and the PP matrix. On the other hand, the much lower experimental value can be seen while the volume content of $Mg(OH)_2$ particles was larger than 0.2. This attributes to the agglomerate of the inorganic particles which destroyed the continuity of PP matrix.

The morphology of PP filled with various amount of $Mg(OH)_2$ composites

The filler dispersion and the phase morphology of neat PP filled with various content of particle were

studied by SEM and shown in Figures 6(a)–6(e). The boundaries and the contrast can be obviously seen between the two phases of $Mg(OH)_2$ particles and PP matrix. The dispersion of filler in PP matrix and the evolvement of morphologies of the incompatible system can be clearly seen in Figure 6. When the content of $Mg(OH)_2$ particles is less than 30 phr, the particle does not affect the integrity of the intersection of PP matrix and this can be seen in Figure 6(a). When the content of $Mg(OH)_2$ particles reach 60 phr, the structure of two phases can be seen, but the particle is relatively even and this can be seen in Figure 6(b). When the content of $Mg(OH)_2$ particles reach 90 phr, particle began to form small agglomerates dispersed in PP matrix and this can be seen in Figure 6(c). When the content of $Mg(OH)_2$ particles reach 120 phr, particles began to form larger agglomerates, which contact each other and this can be seen in Figures 6(d) and 6(e). It is such more and more severely agglomerated particles that cause the larger and larger deviations of the experimental value and the theoretic values of the mechanical properties of composites, besides the bad adhesion.

FTIR study of Zn-SEPDM ionomer

Figure 7 shows the infrared spectra of neat EPDM and zinc neutralized sulfated EPDM with the ion concentration being 0.06 mol/100 g (0.06 mol % Zn-SEPDM). Considering the spectrum (b) of Zn-SEPDM, the band observed at 1026 cm^{-1} was attributed to the S=O stretching mode and the 1221 cm^{-1} band to the asymmetric stretching of S=O. A medium peak at 614 cm^{-1} was associated with the stretching mode of S—O and the band at 1575 cm^{-1} was assigned to the zinc sulfate
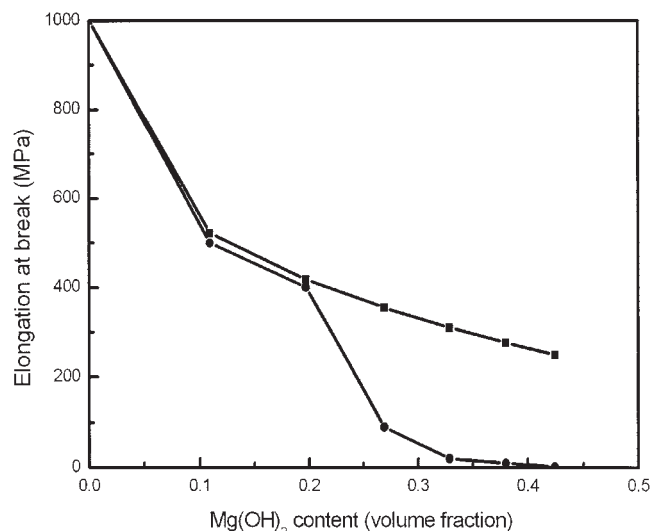

Figure 5 The comparison of theoretic value of Neilsen's model and experimental value of elongation at break of the PP filled with various amount of $Mg(OH)_2$.
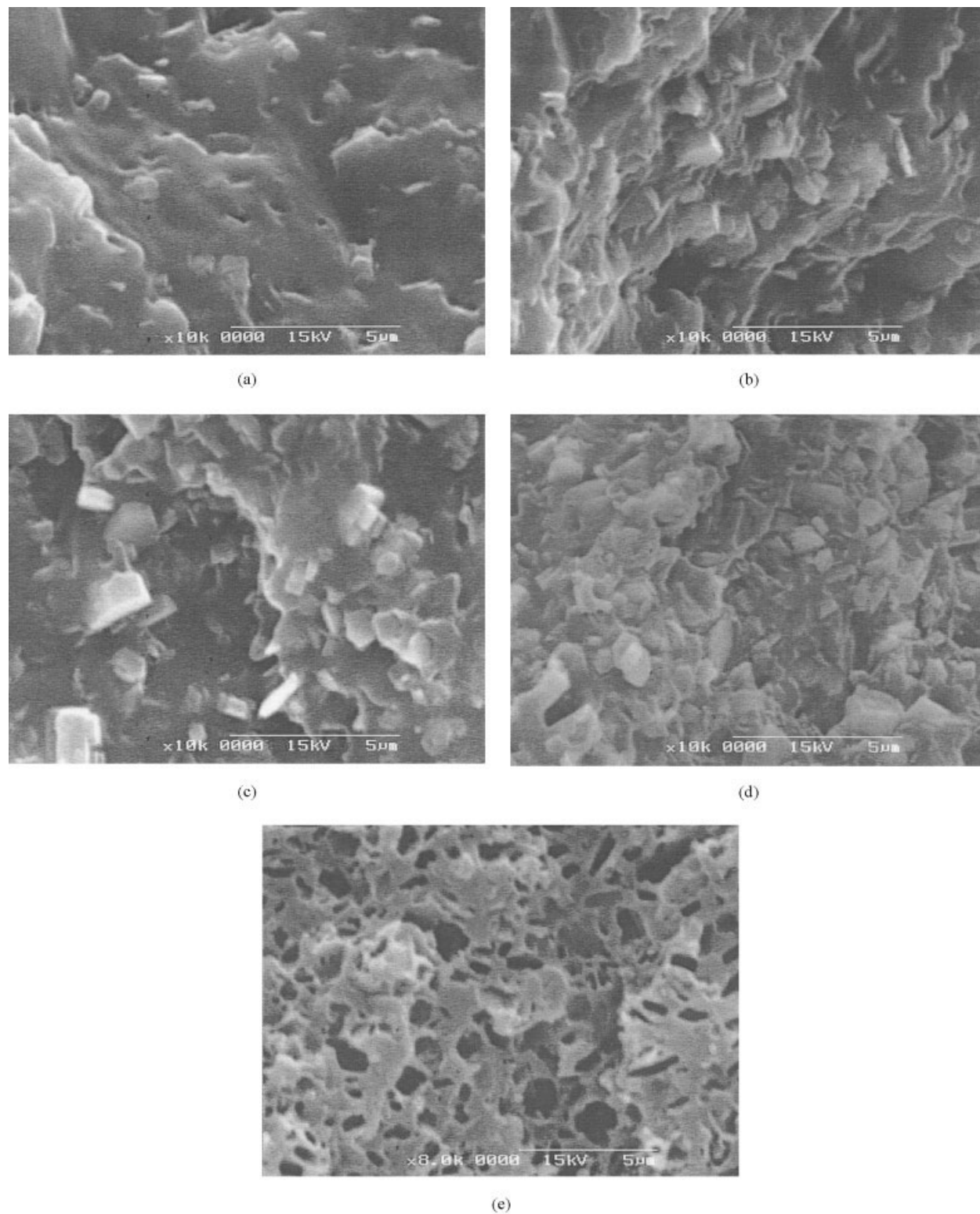
Figure 6 The scanning electron microscopy of the fractured surface of PP filled with various amount of $Mg(OH)_2$. (a) SEM of fractured surface of PP filled with 30 phr $Mg(OH)_2$. (b) SEM of fractured surface of PP filled with 60 phr $Mg(OH)_2$. (c) SEM of fractured surface of PP filled with 90 phr $Mg(OH)_2$. (d) SEM of fractured surface of PP filled with 120 phr $Mg(OH)_2$. (e) SEM of fractured surface of PP filled with 150 phr $Mg(OH)_2$.
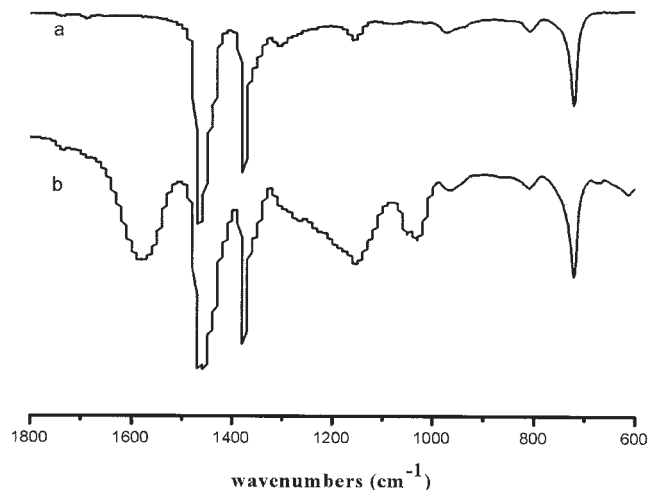
Figure 7 FTIR of neat EPDM and zinc neutralized sulfated EPDM with ion concentration being 0.06 mol/100 g.

Figure 9 The notched Izod impact strength of the PP/EPDM/Mg(OH)$_2$ ternary composites with various amounts EPDM.

ion. The deference between these two spectra certifies that the zinc neutralized sulfated EPDM was obtained by these two-step reactions.[19]

Mechanical properties of ternary composites

Figures 8 and 9 show the effect of EPDM content on the mechanical properties of the PP highly loaded with 140 phr Mg(OH)$_2$ composites. Figures 8 and 9 demonstrated that, using EPDM as the third component, the composites with excellent Izod impact properties can be obtained but with very low strength at break.

The effect of Zn-SEPDM content on the mechanical properties of PP highly loaded with 140 phr Mg(OH)$_2$ composites was shown in Figures 10 and 11. The material with good tensile and impact properties can
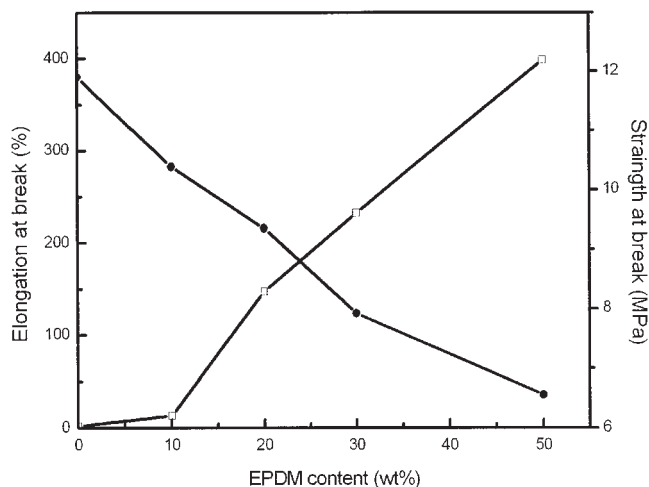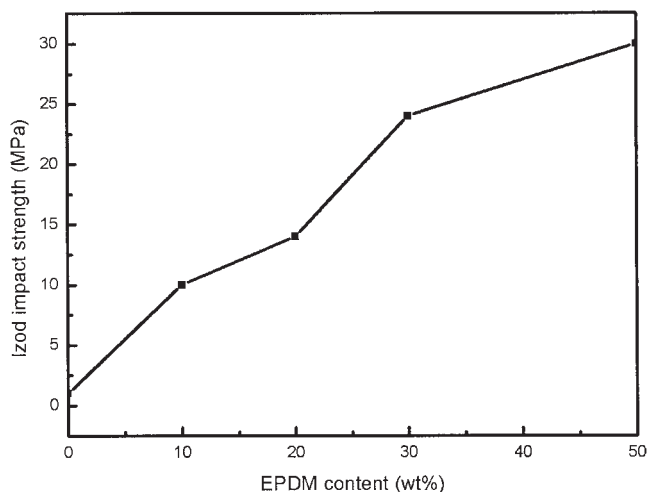
be obtained using Zn-SEPDM as the third component. The changes of mechanical properties observed in the case of PP/Zn-SEPDM/Mg(OH)$_2$ ternary composites is caused by the interfacial adhesion between the rubbery phase and the matrix being better than that of the PP/EPDM/Mg(OH)$_2$ ternary composites, because of ionic interactions by the incorporated ionic groups.[16,19]

The decrease in toughness compared with that of the corresponding PP/EPDM/Mg(OH)$_2$ ternary composites is caused by better interfacial adhesion between the rubbery phase and the matrix. Too much adhesion will affect the interfacial debonding between the modifier and the matrix. On the other hand, the yield stress increases with increasing interfacial adhe-
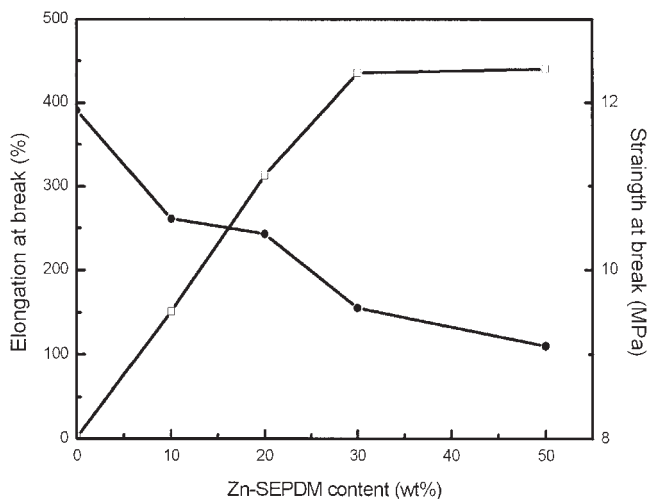

Figure 8 The tensile properties of the PP/EPDM/Mg(OH)$_2$ ternary composites with various amounts EPDM.

Figure 10 The tensile properties of the PP/EPDM/Mg(OH)$_2$ ternary composites with various amounts Zn-SEPDM ionomer.
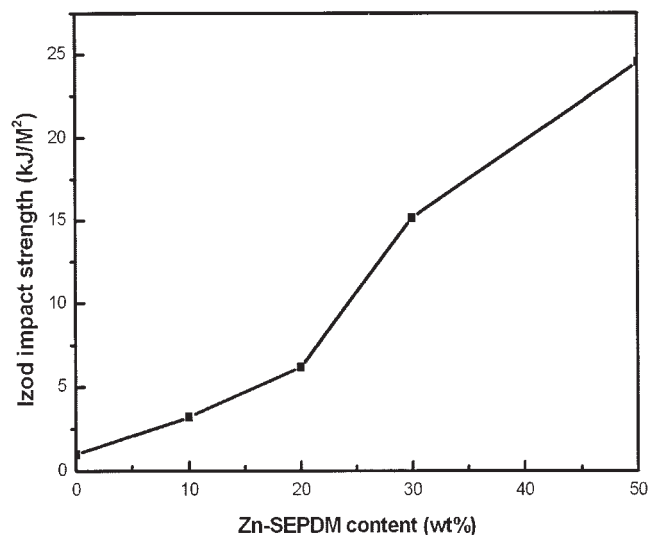
Figure 11 The notched Izod impact strength of the PP/ EPDM/Mg(OH)$_2$ ternary composites with various amounts Zn-SEPDM ionomer.

sion. They all have disadvantages in relation to toughening.

The compatibility between the rubbery phase and the PP matrix play an important role in determining the tensile properties of the composites. Ternary composites with good mechanical properties, toughness, and flame retardant properties consisting of PP, Zn-SEPDM ionomer, and Mg(OH)$_2$ can be obtained.

## Morphology observation of ternary composites

The effects of rubbery phase on the mechanical properties of PP highly filled 150 phr Mg(OH)$_2$ can be illustrated by the dispersion morphology of the filler and rubbery phases. Figures 12(a) and 12(b) show the SEM images of fractured surfaces of PP/EPDM/ Mg(OH)$_2$ and PP/Zn-SEPDM/Mg(OH)$_2$ ternary composites. Obviously, the presence of a few small aggregates can be seen. Nevertheless, the Mg(OH)$_2$ particulates are well dispersed in the matrix. The evenly dispersed Mg(OH)$_2$ particulates embodied the elevated compatibility of the particulates and matrix, because the rubbery phase acted as compatiblizer. The distinction between Figures 12(a) and 12(b) showed the different compatibility feature with different compatiblizer. In PP/EPDM/Mg(OH)$_2$ ternary composites, the much small aggregate of particulates are contacted with each other and confined in partial surface and this can be seen in Figure 12(a). In PP/Zn-SEPDM/Mg(OH)$_2$ ternary composites, the even and discrete dispersion is showed in Figure 12(b).

Figures 13(a) and 13(b) showed the SEM of a fractured surface of PP/EPDM/Mg(OH)$_2$ and PP/Zn-SEPDM/Mg(OH)$_2$ ternary composites after the rubbery phase were removed. The dark region indicates the removed rubbery phase. Very little Mg(OH)$_2$ particulates can be detected demonstrating that those are also removed with the rubbery phased. The conclusion can be that particulates trended to locate in rubbery phase because of its compatibility. PP acted as continuous phase and EPDM or Zn-SEPDM forms the dispersed phase, as can be seen in Figure 13. It appears that the mean size of the domain occupied by the rubbery phase in the order of 0.8 μm to 1.5 μm in PP/EPDM/Mg(OH)$_2$ ternary composites but 0.2 μm to 0.8 μm PP/Zn-SEPDM/Mg(OH)$_2$ ternary composites. The even and discrete dispersion of particulates and the less domain size of rubbery phases showed the better compatibilizer properties of Zn-SEPDM than that of neat EPDM. This also can be explained by the good mechanical performers of PP/Zn-SEPDM/ Mg(OH)$_2$ ternary composites.
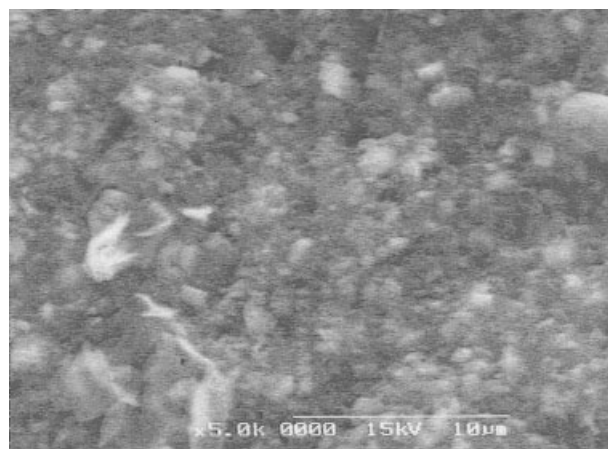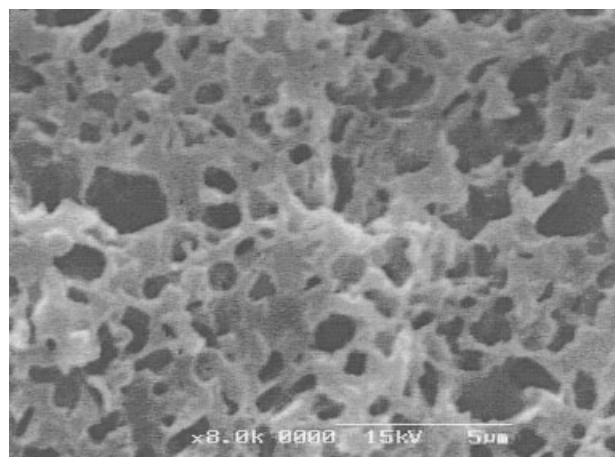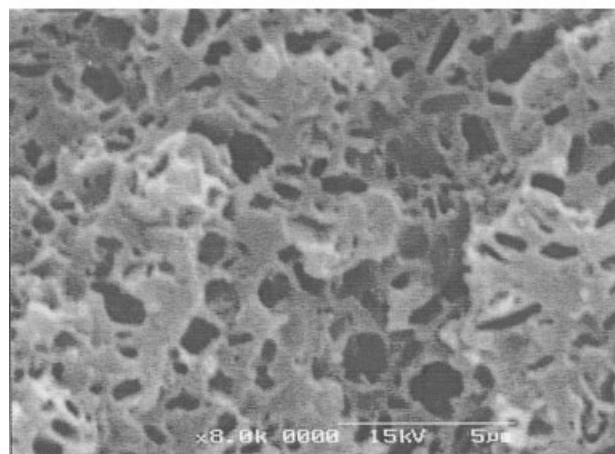

(a)
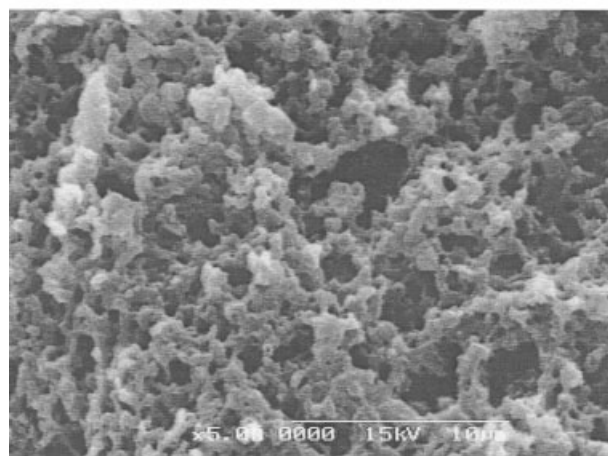
(b)

Figure 12 The scanning electron microscopy of the fractured surface of PP filled with 140 phr Mg(OH)$_2$ composites toughened with 50 phr EPDM or Zn-SEPDM ionomer. (a) SEM of fractured surface of PP/EPDM/Mg(OH)$_2$ ternary composite. (b) SEM of fractured surface of PP/Zn-SEPDM/ Mg(OH)$_2$ ternary composite

Figure 13 The scanning electron microscopy of the fractured surface of PP filled with 140 phr $Mg(OH)_2$ composites toughened with 50 phr EPDM or Zn-SEPDM ionomer after the rubbery phases being etched. (a) SEM of fractured surface of PP/EPDM/$Mg(OH)_2$ ternary composite. (b) SEM of fractured surface of PP/Zn-SEPDM/$Mg(OH)_2$ ternary composite.

CONCLUSIONS

1. PP was endowed with excellent flame retardant properties by great mount of $Mg(OH)_2$ particulates.
2. It was found that the bad compatibility between filler and matrix and the nonlinear agglomerate of $Mg(OH)_2$ particles in PP matrix caused the severe deterioration of composites.
3. The addition of rubbery phase as the third component could remarkably improve the Izod impact strength of highly filled PP. The composites possessed better mechanical properties using sulfated EPDM ionomer as the third component than that of neat EPDM.
4. The theoretical analysis and SEM photographs showed that even and discrete dispersion of particulates and the less domain size of rubbery phases as well as the better adhesion between rubbery phase and PP matrix were the main reasons for explaining the improvement of the mechanical properties.

References

1. Gonzalez, J.; Albano, C.; Ichazo, M.; Diaz, B. Eur Polym Mater 2002, 38, 2465.
2. Dolakova-Svehlova, V. J Macromol Sci Phys B 1982, 21, 231.
3. Dolakova, V.; Hudecek, F. J Macromol Sci Phys B 1978, 15, 337.
4. Titelman, G. I.; Gonen, Y.; Keidar, Y.; Bron, S. Polym Degrad Stab 2002, 77, 345.
5. Sain, M.; Park, S. H.; Suhara, F.; Law, S. Polym Degrad Stab 2004, 83, 363.
6. Zhu, S.; Zhang, Y.; Zhang, Y. X. Polym Polym Comps 2002, 10, 447.
7. Wang, G. L.; Jiang, P. K.; Zhu, Z. K.; Yin, J. J Appl Polym Sci 2002, 86, 2544.
8. Tai, C. M.; Li, R. K. Y. J Appl Polym Sci 2001, 80, 2718.
9. Wang, G. L.; Jiang, P. K.; Zhu, Z. K.; Ying, J. J Appl Polym Sci 2002, 85, 2485.
10. Wu, S. H. Polym 1985, 26, 1855.
11. Kim, G. M.; Michler, G. H. Polym 1998, 39, 5699.
12. Gonzalez-Montiel, A.; Keskkula, H.; Paul, D. R. Polym 1995, 24, 4621.
13. Xie, X. L.; Li, R. K. Y.; Liu, Q. X.; Mai, Y. W. Polym 2004, 45, 2793.
14. Dompas, D.; Groeninckx, G.; Isogawa, M.; Hasegawa, T.; Kadokura, M. Polym 1995, 36, 437.
15. Jeon, H. S.; Oh, S. H.; Kim, J. S.; Lee, Y. Polym 2003, 44, 4179.
16. Dreyfus, B. Macromol 1985, 18, 284.
17. Tadano, K.; Hirasawa, E.; Yamamoto, H.; Yano, S. Macromol 1989, 22, 226.
18. Xu, L.; Weiss, R. A. Macromol 2003, 36, 975.
19. Su, Z. P.; Jiang, P. K.; Li, Q.; Wei, P.; Wang, G. L.; Zhang, Y. J Appl Polym Sci 2004, 94, 1504.
20. Lopez-Manchado, M. A.; Kenny, J. M.; Quijada, R.; Yazdani-Pedram, M. Macromol Chem Phys 2001, 202, 1909.
21. Mokrini, A.; Acosta, J. L. Polym 2001, 42, 9.
22. Neilsen, L. E. J Appl Polym Sci 1966, 10, 97.
23. Dolakova-Svehlova, V. J Macromol Sci Phys B. 1982, 21, 231.